

Journal of Biomedical Optics

SPIEDigitalLibrary.org/jbo

R and G color component competition of RGB image decomposition as a criterion to register RBC agglutinates for blood group typing

Valeri A. Doubrovski
Yuliya A. Ganilova
Igor V. Zabenkov

R and G color component competition of RGB image decomposition as a criterion to register RBC agglutinates for blood group typing

Valeri A. Doubrovski,* Yuliya A. Ganiylova, and Igor V. Zabenkov

Saratov State Medical University named after V.I. Razumovsky, Department of Medbiophysics, 112. Kazachaya Street, 410026 Saratov, Russia

Abstract. A new approach of the criterion assignment for registration of erythrocyte agglutinates to instrumentally determine blood group type is suggested. The criterion is based on comparison of R and G components of RGB decomposition of microscopy digital image taken for the blood-serum mixture sample. For the chosen experimental conditions, the minimal size (area) of RBC agglutinate to be registered by the criterion suggested is estimated theoretically. The proposed method was tested experimentally on the example of monitoring agglutinates in flow. The encouraging experimental results were obtained for improvement of the resolving power of the method; the optimal experimental conditions were revealed for maximum resolution. Though the suggested method was realized for dynamic (flow) blood group determination, it could also be applied for diagnostics in a stationary environment. This approach increases the reliability of RBC agglutinates registration and, hence, blood group typing. The results may be used to develop the apparatus for automated determination of human blood group. © 2014 Society of Photo-Optical Instrumentation Engineers (SPIE) [DOI: 10.1117/1.JBO.19.3.036012]

Keywords: blood group typing; erythrocytes agglutination; flow method; digital microimages; RBC decomposition; correlation analysis.

Paper 130379RRR received May 30, 2013; revised manuscript received Jan. 27, 2014; accepted for publication Jan. 28, 2014; published online Mar. 17, 2014.

1 Introduction

Blood group typing is one of the most frequent diagnostic tests in medical laboratory practice: Thus, in the United States alone, 150 to 200 million tests are performed annually to determine the blood groups in blood centers.¹ A large number of such tests to be performed annually requires the development of apparatus for automatic blood typing.

There are many similar devices available in the market; some of them are presented in Table 1.

These devices are based on different physical principles; they are widely used in medical laboratory diagnostics, but the problem to improve the characteristics and abilities of the devices for instrumental blood typing remains relevant. Many investigators make attempts to increase reliability of flow, see, for example, Refs. 1 to 12, or static^{13–23} methods for blood group determination, as well as to find the related biomedical problems that could be solved by these methods and instruments.

The process of erythrocytes agglutination is the basis of many medical diagnostic tests and partially blood group typing. Let us recall that agglutination takes place in the case when agglutinating serum corresponds immunologically to erythrocytes of a given blood group sample (positive reaction, the agglutinates are formed). Otherwise RBC agglutination is absent; erythrocytes remain not glued (free)—negative reaction.

The aim of any device for blood typing, including that mentioned in Table 1, is to get maximum difference (as a rule ratio) of the parameters measured for the case of positive reaction in respect to the same parameter for the negative one. The combination of these two parameters is usually named as the resolving power of apparatus r . The higher resolution of the device means

the higher reliability of blood group typing. It is important to notice that the basic specificity of the devices for blood typing is the fact that the mistake is to be excluded absolutely. Otherwise different sad results may happen during patient's blood transfusion up to a lethal one.

That is why the developers of apparatus for blood typing are to introduce some criteria (threshold levels) r_1 and r_2 . For example, if the parameter r of the device is higher than the threshold level r_1 chosen and introduced by the designer of the device, then one may believe that the reaction of agglutination is positive. If $r < r_2$, then the reaction is negative. Finally, if r is in the corridor $r_2 \leq r \leq r_1$, then the apparatus makes it possible to answer "blood group type is not determined." It is much better not to define blood type than to make a mistake. For the last case, additional investigations are to be fulfilled by means of cross-methods or manually.

Let us present some cases of such an approach. The results of testing of the device for blood typing developed by Chung et al.²⁴ were compared with the results of ABO and Rh analyses made in parallel on the basis of Technicon AutoAnalyzer and in some cases by a manual technique (not instrumental one). The comparison showed that in 97.3% of cases (10,042 blood samples), both devices determined blood group types of the samples and they answered "the group type is not determined" in 266 cases only. For these cases, the type of blood was determined manually by inverse testing of cross-method.

In Ref. 25, the device Inverness Blood Grouping System (IBG System) was tested in an analogical way as in Ref. 24, and the results of instrumental measurements were compared with manual ones. In three cases only, out of 2051, the results

*Address all correspondence to: Valeri A. Doubrovski, E-mail: doubrovski43@yandex.ru

Table 1 The apparatus for blood typing.

Apparatus	Firm	Country
Galileo Echo™	ImmucorGamma	USA
PK7200® Automated Microplate System	Olympus Diagnostics	Japan
TANGO Benchtop Blood Bank Analyzer		
ORTHO AUTOVUE Innova/Ultra System	Ortho-Clinical Diagnostics	USA
ORTHO ProVue™ Automated BloodBank Instrument	Johnson & Johnson company	
Automatic analyzer WADiana Compact	Diagnostic Grifols S.A.	Spain
Auto Analyzer	Technicon Instrument Corporation	USA
Groupamatic	Centre National de Transfusion	France
Haemotyper	Tecan	Switzerland

obtained by the IBG System were different from the manual ones.

It is important to notice that the criteria (threshold levels) may be introduced in different ways; this depends upon the construction of the devices. For example, in PK7200® Automated Microplate System (Olympus), such a criterion is the shape of images of sediments for negative and positive reactions on the bottom of the cuvette with a special bottom profile. The pattern of cells/agglutinates distribution on the cuvette bottom (so-called pattern of agglutination) was analyzed by digital method; it gave the opportunity to differ positive reaction from negative one.

The authors of Refs. 13 and 14 after authors of Refs. 15 and 16 introduced a criterion as the ratio of the spectral characteristic slopes for the sample under analyses (mixture of blood-serum, positive reaction) and the sample for control (negative reaction) in the range of optical testing in the wavelength range of 665 to 1000 nm. In this range, the spectral characteristics are linear and the difference of their slopes has maximum;^{13–16} this parameter was named by the authors as “index of agglutination.” Numerous investigations and corresponding statistic estimations led them^{13–16} to the magnitude of the criterion $r_{cr} = 17$: if $r \geq r_{cr}$, then one is to assume that positive reaction had taken place.

In Ref. 17, the resolving power of blood typing method was defined as a ratio of two photoelectric signals (intensities) $r = I_+/I_-$ accepted by the receiver, where I_+ corresponded to positive reaction and I_- to the negative one. The higher r blood group typing is more reliable.

In the same way, in Refs. 18 and 19, r was treated as a ratio of two levels of brightness for blood-serum mixture images at a chosen moment of cells sedimentation for positive and negative reactions of agglutination.

The authors of Refs. 11 and 12 investigated the possibility to use the correlation analysis for the problem of blood typing. They used the integrated value of correlation coefficient to compare positive and negative reactions.

The investigation presented here is focused on the development of a new approach to introduce the criterion of registration RBC agglutinates with the aim of instrumental blood typing. The work is based on the application of optical spectral features of blood and probing light beam on one hand and R and G component competition of RGB decomposition of blood-serum mixture image of sample under study on the other hand. Such an approach gives an opportunity to compare the areas of digital images of agglutinates (positive reaction) and some RBC formations (negative reaction). The investigation is aimed to increase the reliability of human blood group determination.

2 Theoretical Description

Our observations showed that for positive reaction of agglutination enhanced by ultrasound,^{17,22,23} the erythrocyte immune complexes occur to be so large that they contain from several erythrocytes up to many tens and even hundreds of cells. At the same time, for negative reaction the mixture blood–serum presents a single red blood cell suspension (Fig. 1). Figure 1 shows a great effect of ultrasonic standing wave (USW) application on formation of RBC agglutinates. The USW application to blood group testing was discussed in Refs. 17, 22, and 23; it will be analyzed in Sec. 3.1.

Naturally, both agglutinates or free erythrocytes absorb and scatter light beams with different wavelengths in different ways. Let us consider consistently the probe light beams transport through the layers of packed RBC (PRBC) (the model of immune complex, positive reaction of agglutination) or through blood solution (negative reaction). In both cases, the probe light beam will be treated in two ways:

- Dual-wavelength light beam (Sec. 2.1)
- Spectrally filtered testing light beam (Sec. 2.2).

Finally, for both types of probe optical beams R and G, components of RGB decomposition of blood-serum mixture sample images will be analyzed.

2.1 Dual-Wavelength Probing of Blood-Serum Mixture

Let us demonstrate the principle of RBC agglutination registration by two-wavelength probing of blood-serum mixture. The PRBC of blood layer is assumed to be probed by two monochromatic light beams with different wavelengths of the visible range λ_1 and λ_2 . Hemoglobin spectrum (one of the constituents of RBC content) is presented in Fig. 2 (curve 1).

Wavelengths λ_1 and λ_2 are chosen according to hemoglobin spectrum: $\lambda_1 = 540$ nm corresponds to one of the maxima of absorption in green range of spectrum and $\lambda_2 = 640$ nm corresponds to that when light absorption is much lower. Estimations based on the Twersky formula²⁶ show that the attenuations of light beams at λ_1 and λ_2 due to scattering phenomenon should be quite close to each other because scattering cross-sections for erythrocytes for both wavelengths are nearly equal. At the same time, the attenuation of light beams at λ_1 and λ_2 differs, and this difference increases when RBC concentration and/or blood layer thickness increases. This allows one to assume that light beams at λ_1 and λ_2 , which pass through the sample, are attenuated mostly due to absorption phenomenon; this may be described by Bouguer’s law:

$$I(\lambda_1) = I_0(\lambda_1) \exp[-\mu_a(\lambda_1)l], \quad (1)$$

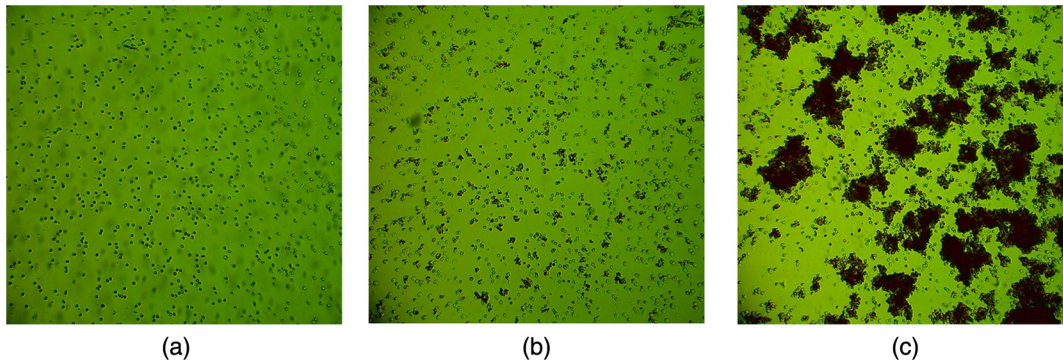


Fig. 1 Fragments of microscopic images: erythrocytes (negative reaction of agglutination) (a); erythrocytes and their immune complexes (agglutinates, positive reaction) (b) and with US irradiation of mixture (c).

$$I(\lambda_2) = I_0(\lambda_2) \exp[-\mu_a(\lambda_2)l], \quad (2)$$

where $I(\lambda_1)$ and $I(\lambda_2)$ are the light beam intensities at λ_1 and λ_2 at the output of the blood layer; $I_0(\lambda_1)$ and $I_0(\lambda_2)$ are the intensities of light beams falling down upon the sample; $\mu_a(\lambda_1)$ and $\mu_a(\lambda_2)$ are the absorption coefficients of hemoglobin at λ_1 and λ_2 , respectively; l is the thickness of the sample.

The absorption coefficient $\mu_a(\lambda)$ may be defined as follows:²⁷

$$\mu_a(\lambda) = (2.3eC)/(64,500), \quad (3)$$

where e is the molar light absorption coefficient for hemoglobin [(1/cm)/(mole/l)] and C is the hemoglobin concentration (g/l); molecular weight of hemoglobin is 64,500 (g/mole). The values of $e(\lambda)$ and C can be found in Ref. 27. For whole blood, C is equal to 150.

Taking into account that the PRBC sample has a higher concentration of erythrocytes related to the whole blood, it is necessary to correct Eq. (3) in respect to Ref. 27 by introducing hematocrit H (assuming that when plasma is totally deleted from blood after blood centrifugation, $H = 1$). In addition, in order to account for PRBC sample dilution, parameter N was introduced. Correspondingly, Eq. (3) is transformed to

$$\mu_a(\lambda) = (2.3e150/HN)/(64,500). \quad (4)$$

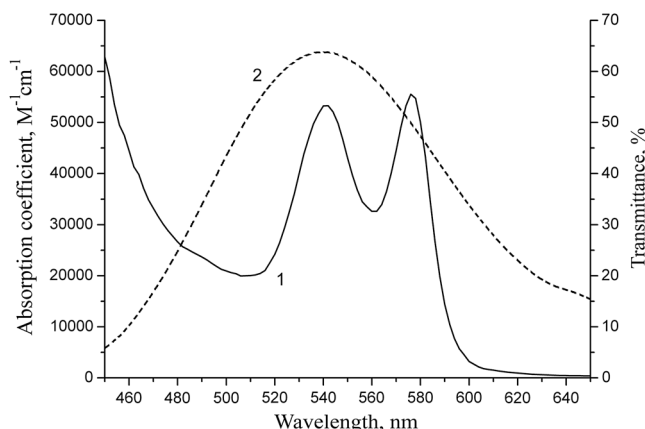


Fig. 2 Spectral characteristics: 1—hemoglobin, 2—optical filter.

The estimations using Eq. (4) for $C = 150$, $e(\lambda_1) = 53,236$, $e(\lambda_2) = 4$ [oxyhemoglobin, (1/cm)/(mole/l)²⁷], $H = 1/2$, and $N = 1$ (no dilution) give the following results: $\mu_a(\lambda_1) = 575(\text{cm}^{-1})$, $\mu_a(\lambda_2) = 4(\text{cm}^{-1})$. The calculated dependences for $\mu_a(\lambda_1)$ and $\mu_a(\lambda_2)$ are presented in Fig. 3 (curve 1 corresponds to $\lambda_1 = 540$ nm and curve 2 to $\lambda_2 = 640$ nm); the ratio of intensities $K = I_0(\lambda_1)/I_0(\lambda_2)$ was chosen as $K > 1$. It is important to notice that the curves 1 and 2 are crossing in the point I_0 , which corresponds to such a PRBC layer thickness when $I(\lambda_1) = I(\lambda_2)$. From the graphs, it is obvious that for $K = 4.3$ (the K value will be discussed in Sec. 3), the layer thickness is $l_0 = 26 \mu\text{m}$. A similar result can be obtained analytically.

$$l_0 = \ln K / [\mu_a(\lambda_1) - \mu_a(\lambda_2)]. \quad (5)$$

Notice that Eq. (5) is derived from Eqs. (1) and (2) taking into account $I(\lambda_1) = I(\lambda_2)$.

From Fig. 3 it is easy to see (curves 1 and 2) that for sample layer thickness $l < l_0$, the relation between intensities is $I(\lambda_1) > I(\lambda_2)$ —the green spectrum component prevails over

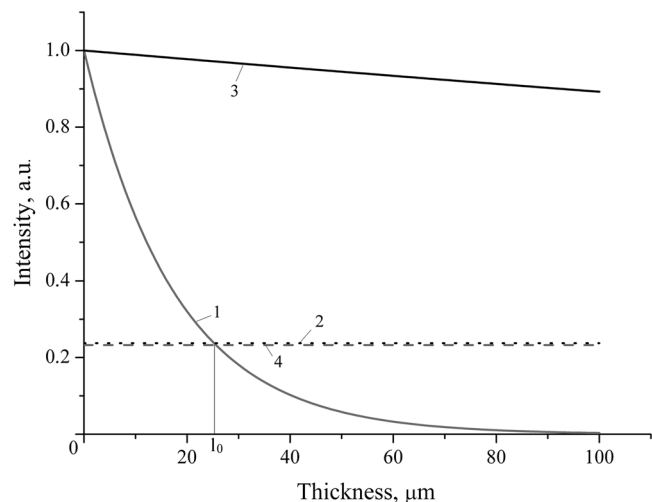


Fig. 3 The intensity of light flux at the output of blood layer as a function of its thickness: erythrocyte mass—1 corresponds to $\lambda_1 = 540$ nm and 2 to $\lambda_2 = 640$ nm; erythrocyte mass solution—3 corresponds to $\lambda_1 = 540$ nm and 4 to $\lambda_2 = 640$ nm. The level of erythrocyte mass dilution was 1:150.

red one when PRBC sample is probed by dual-wavelength beams. Otherwise, for $l > l_0$, the blood layer thickness becomes so large that in spite of the accepted condition $K > 1$, the relation between intensities is $I(\lambda_1) < I(\lambda_2)$, i.e., the red spectral component dominates. This result may be related to the case of positive reaction of agglutination when erythrocytes are glued by serum, and this clot is similar to PRBC blood sample.

These estimations and data presented in Fig. 3 permit to formulate the following approach for registration of immune RBC complexes. If in blood-serum mixture being tested by dual-wavelength optical probe large erythrocyte formations of red color are visualized ($l > l_0$), then they may be treated as RBC agglutinates (positive reaction).

Let us consider the model of negative reaction of agglutination. In this case, there are no agglutinates; sample is a suspension of erythrocytes in saline. For the experimental blood dilutions from (1:300) to (1:50), the level of N was varying within the limits $50 \leq N \leq 300$ (will be discussed in Sec. 3). The calculations using Eqs. (4) and (5) give the following values $1.3 \leq l_0 \leq 7.8$ (mm). In the experiments the blood layer thickness l was 0.3 mm (Sec. 3), i.e., $l < l_0$; hence, $I(\lambda_1) > I(\lambda_2)$ and the blood layer image will be always green. It is easy to see the same from Fig. 3: the curves 3 and 4 do not intersect. Then it is possible to state that if sample image is green then agglutination has not been taken place (negative reaction).

On the whole, the generalization of the cases for positive and negative reactions of agglutination leads to the following criterion:

- The agglutination reaction is positive if there are some formations of red color in the sample image; they may be counted as agglutinates.
- The agglutination reaction is negative if sample image appears in green color and red formations are not observed.

2.2 Sample Testing by a Spectrally Filtered Light Beam

The difference between the problems studied here and in Sec. 2.1 lies in the fact that the probing light beam is not the combination of two monochromatic waves now, but a light beam with a continuous spectrum passed through an optical filter. Furthermore, if in Sec. 2.1 in order to find the critical thickness of blood layer l_0 , two intensities of light beams compared at the wavelengths λ_1 and λ_2 were equalized [$I(\lambda_1) = I(\lambda_2)$], in this section the same parameter l_0 will be estimated by the comparison of R and G components of RGB decomposition of sample image [$B(R) = B(G)$]. Hereinafter, the following designations are accepted: $B(B)$, $B(R)$, and $B(G)$ are the brightness of blue/red/green components of the image.

In the experiments, the source of light illumination of a sample was a filament lamp (Biomed microscope, Sec. 3), the spectrum of which is close to the spectrum of ideal black body at a temperature 3000 K. This light was transported through optical green filter. Its spectrum is presented in Fig. 2. One should pay attention to the fact that maximum of its light transmittance is very close to one of light absorption spectrum maxima for hemoglobin in the green range ($\lambda \approx 540$ nm).

To find erythrocyte layer thickness l_0 , when brightness of red component $B(R)$ and green one $B(G)$ become equal, a rigorous approach is used: it is based on the calculation of XYZ

coordinates of the sample in a linear color coordinate system and then on color transformation from XYZ to RGB. To estimate X,Y,Z color components, the spectral characteristics of the following were used: light source spectrum, $S(\lambda)$, optical filter spectrum, $F(\lambda)$, and spectral coefficient of transmission of PRBC of blood dependence, $T(\lambda)$, which were calculated on the basis of data for $\mu_a(\lambda)$ from Sec. 2.1. Still, as in Sec. 2.1, it is assumed that light beam attenuation is caused by light absorption only; the wavelength-dependent changes of light scattering in the sample in the visible range are not significant. Thus, the final formula to calculate color coordinates X , Y , and Z for the sample is as follows:

$$\begin{aligned} X &= k \int_{\lambda} \bar{x}T(\lambda)F(\lambda)S(\lambda)d\lambda, & Y &= k \int_{\lambda} \bar{y}T(\lambda)F(\lambda)S(\lambda)d\lambda \\ Z &= k \int_{\lambda} \bar{z}T(\lambda)F(\lambda)S(\lambda)d\lambda, \end{aligned} \quad (6)$$

where \bar{x} , \bar{y} , and \bar{z} are the sensitivity functions, k -coefficient of normalization. The subsequent conversion from color space XYZ into RBG was carried out by means of multiplication of transforming matrix M (the source of irradiation is of A type) by vector column made up of components of color space XYZ.

$$\begin{pmatrix} R \\ G \\ B \end{pmatrix} = M \begin{pmatrix} X \\ Y \\ Z \end{pmatrix}. \quad (7)$$

Equations (6) and (7) allow one to estimate R, G, and B color components of RGB decomposition of image by varying the wavelength of light λ in the limits $360 \leq \lambda \leq 830$ nm for a chosen thickness of blood layer l . Taking different values of l and fulfilling the same calculations for each l , one may get the critical blood layer thickness l_0 when brightness of $B(R)$ and $B(G)$ components are equal [$B(R) = B(G)$]. The calculations showed that $l_0 = 27.2 \mu\text{m}$, which is very close to the result obtained in Sec. 2.1.

Comparison of the results obtained in Secs. 2.1 and 2.2 shows that the criterion suggested to register RBC agglutinates may be realized in practice in two modes of light beam probing of blood-serum mixture:

- Dual-wave radiation as an optical probe, for example, two lasers or light-emitting diodes with different, but specially chosen wavelengths and intensities.
- A single testing light beam, but with a specially spectral filtered radiation.

3 Experiment

3.1 Sample Preparation Technique

As noted in Sec. 2.1, the sample under study is erythrocyte mass of donor blood for all four groups in ABO system. In this paper, such a sample will be named as erythrocyte mass or the sample of blood or simply blood.

Blood was diluted by saline and then agglutinating serum was added. Taking into account the serum volume, the blood (PRBC) dilution was 1:25 and the ratio of blood-serum was 1:10, which is the standard proportion for medical diagnostic

practice when whole blood is investigated, but not for PRBC blood samples. As an example, let us recall that the combination blood A(II)-serum A_{β} (II) does not lead to RBC agglutination (negative reaction), but the same blood sample mixed with serum B_{α} (III) leads to immune erythrocyte complexes formation (agglutinates)—positive reaction of agglutination.

It was shown in Refs. 17, 22, and 23 that ultrasonic standing wave (USW) action upon blood-serum mixture leads to agglutination reaction intensification, which increases the quantity of immune erythrocytes complexes and, most important, their sizes. The tested blood-serum mixture was poured into the cuvette of 6 ml in volume and then it was placed on piezoceramic transducer. Ultrasonic frequency was 2.25 MHz and voltage not more than 15 V in order to avoid RBC hemolysis. To optimize sample preparation technique, time duration of ultrasonic action upon sample was varied discretely in the limits from 15 s up to 2 min.

USW oriented in vertical direction grouped erythrocytes in its nodal zones. That led to the cell stratification in liquid with a period equal to a half of ultrasonic wavelength ($\lambda_{us}/2$). The erythrocyte convergence in the nodal zones of USW increased the probability of their induced aggregation (agglutination). In the presence of immunologically adequate serum, erythrocytes were gluing (agglutinating) and large immune RBC complexes were forming—positive reaction of agglutination. These complexes and free (not glued) erythrocytes were levitating—they remained weightless due to USW action. When ultrasound was switched off, large and rather stable RBC agglutinates were sedimenting quickly.

At the same time, when blood sample tested was not immunologically adequate to the type of serum (negative reaction), the formation of agglutinates in the nodal zones of USW did not occur. Under this condition, unstable RBC aggregates were formed: they fell into individual cells when ultrasound was switched off. It is necessary to notice that the rate of RBC sedimentation was much lower than that for agglutinates. USW action upon the mixture blood-serum was analyzed in Refs. 22 and 23.

So after some time (the duration of sample incubation) due to the difference in the rates of sedimentation, the agglutinates for positive reaction or free erythrocytes for negative one accumulate on the bottom of the cuvette. It should be noticed that blood-serum mixture incubation is an interval of time from the moment of ultrasound switching off up to the moment when sediment of liquid under test is sampled. Then sediment was diluted by saline. The process of incubation was necessary to form the sediment enriched by agglutinates for positive reaction as the negative one did not lead to the formation of agglutinates. To find the optimal time of incubation, it was varied in experiments discretely in the limits from 15 s up to 4 min. After incubation for both types of reactions, equal volumes of liquid investigated (2 ml) being taken from the cuvette bottom were diluted in such a proportion to provide the final blood dilution discretely from 1:300 to 1:50. These solutions of agglutinates (positive reaction) or erythrocytes (negative reaction) were transported through a capillary with cross-section $0.3 \times 1.5 \text{ mm}^2$ and analyzed by a digital microscopy method.

3.2 Experimental Device, Imaging of the Sample

The experimental device was based on optical microscope Biomed, WEB-camera Logitect-QuickCam connected to computer. All the settings of WEB-camera were fixed; they were not changed during the series of experiments. Hereinafter,

WEB-camera used will be named as digital camera. Light beam from filament lamp (microscope illuminator) passed through green glass filter (supplied microscope); its spectral characteristic measurement is presented in Fig. 2 (curve line 2). From Fig. 2, it is easy to see that for the filter used and for the wavelengths chosen in Sec. 2 ($\lambda_1 = 540 \text{ nm}$ and $\lambda_2 = 640 \text{ nm}$), the ratio $K = I_0(\lambda_1)/I_0(\lambda_2)$ is 4.3.

Then light beam being filtered was directed on the glass capillary with a rectangular cross-section of $0.3 \times 1.5 \text{ mm}^2$ through which the liquid under investigation was pumping. In contrast to Ref. 12, microscope objective was changed from 40 \times to 20 \times and ocular from 10 \times to 15 \times because it was revealed experimentally that in the tested liquid flow heavy large immune erythrocyte complexes were moving along the bottom of microcapillary. The application of objective with a longer working distance (magnification 20 \times) allowed for focusing microscope optical system on the bottom of capillary and to detect large agglutinates. The ocular change was necessary to keep the level of microscope magnification.

The digital camera Logitect-QuickCam was able to make 15 shots per second. For each sample, the liquid flow was registered: video-clip of 150 frames was made. It is very important to notice that on the computer monitor large immune erythrocyte complexes were red in color [Fig. 1(c)], but free erythrocytes and small complexes were dark green [Figs. 1(a) and 1(b)], as it was predicted in Sec. 2. Naturally, the color cannot be seen in the black-and-white images (Fig. 1): erythrocytes and their small agglutinates appear black with respect to the background; they can be differentiated from each other in size only.

4 Principles of Computer Processing of RBCs and Their Immune Complex Microimages

In this study, the comparison of the results for different types of interaction of blood samples with serum was carried out by means of agglutinates image capture and determination of their sizes (areas of their images) for positive reaction and, at the same time, by fixing practical absence of agglutinates for negative one. In the latter case, the size of agglutinates should be equal to zero. Naturally, such a processing of experimental results was based on the criterion suggested in Sec. 2, which is connected with the comparison of R and G components of RGB decomposition of the sample image.

4.1 Binarization of RBCs and Their Immune Complex Images

The first step in the experimental results processing was the procedure of video images binarization: it simplifies the agglutinates area calculation by the computer program. Binarization of the raw digital images was fulfilled by RGB analysis. Two digital matrixes B(R) and B(G) corresponding to the image were compared pixel by pixel programmatically. If brightness B(G) corresponding to a definite pixel of the image was higher than B(R) in the same point of image frame, then B(R) was zeroed [B(R) = 0]. Otherwise brightness B(R) was assigned to the definite numerical value, for example, 255.

For negative reaction when the sample contains free erythrocytes only, the condition B(G) > B(R) (according to Sec. 2) for each pixel leads to B(R) = 0 in every point of the binarized image, i.e., the image is black completely.

For positive reaction in the areas of the image frame corresponding to intracellular space, free erythrocytes, or small RBC immune complexes, the condition $B(G) > B(R)$ is fulfilled, and thus, these zones were formatted as black. However, in other areas of the frame, where large RBC immune complexes are placed, it appears $B(G) < B(R)$ and the brightness $B(R)$ is assigned to a number, for example, 255. This area in monitor is colored in red (hereinafter on the black-and-white illustration this zone is marked as gray).

As a result, the comparison of components of image brightness $B(G)$ and $B(R)$ allows one to transform the raw sample image into a binary one. We have to note that

- an erythrocyte agglutinate has a volumetric structure and the comparison of image brightness $B(G)$ and $B(R)$ is based on light transport through it; but taking into account that the image is flat, it is assumed that the size of agglutinate is presented by its area in the image;
- binary image area does not cover the area of real image of a real object; it may be treated as an approximation only.

But (as will be illustrated later in Sec. 5) such an approach is quite acceptable to register RBC agglutinates.

For clarity, quantitative confirmation of the effect observed, and illustration of the binarization result, Fig. 4 is presented. In Fig. 4(a), one can see the images of a single erythrocyte (I) and four RBC immune complexes of different sizes (II to V).

For agglutinates III to V, white outline selects the zones of red color; the rest of the external to the outline is of dark green color. In the selected areas of agglutinates, the thickness of the agglutinates (perpendicular to the picture plane) is high enough to provide light beam at $\lambda_1 = 540$ nm to be absorbed completely, while the beam at $\lambda_2 = 640$ nm due to small

absorption coefficient is passing through this agglutinate freely. That is why agglutinate looks red. At the same time, a single erythrocyte (I, its thickness is $2 \mu\text{m}$ only) and a small RBC immune complex (II) have dark green color.

Brightness as a function of coordinate X along the line L-L' is presented in Fig. 4(b) for five raw images (I to V) of Fig. 4(a). From Fig. 4(b), it is easy to observe that there are regions (marked by crosses) where $B(R) > B(G)$, only for the cases III to V. It is important to note that for these regions only [Fig. 4(b)], there are red zones in Fig. 4(a). It is interesting that brightness distribution $B(X)$ corresponds not only to the size of erythrocyte, but to its shape as well.

4.2 Calculation of RBC Agglutinate Area

To obtain data on the number of agglutinates and their areas from binary images of raw microimage, the procedure of image segmentation was used on the basis of principles of splitting and merging. As a result of such an approach, the location and area of each agglutinate were determined. In calculations, in order to take into account the areas of agglutinates, only selection of sample image structures by areas was carried out. If the area of the structure is less than the threshold S_0 [S_0 corresponded to the maximal size (area) of a single erythrocyte], the blood structure element was assumed as an RBC and information about it was not taken into consideration. But when the area of the blood structure was greater than or equal to S_0 , this element was prescribed as an agglutinate and its area was written down in file. It is important to note that in the case of negative reaction, erythrocytes in flow may become located occasionally close to each other; we named such RBC groups as RBC-formations. They may be accepted by blood typing apparatus as agglutinates. Let us introduce the following notations:

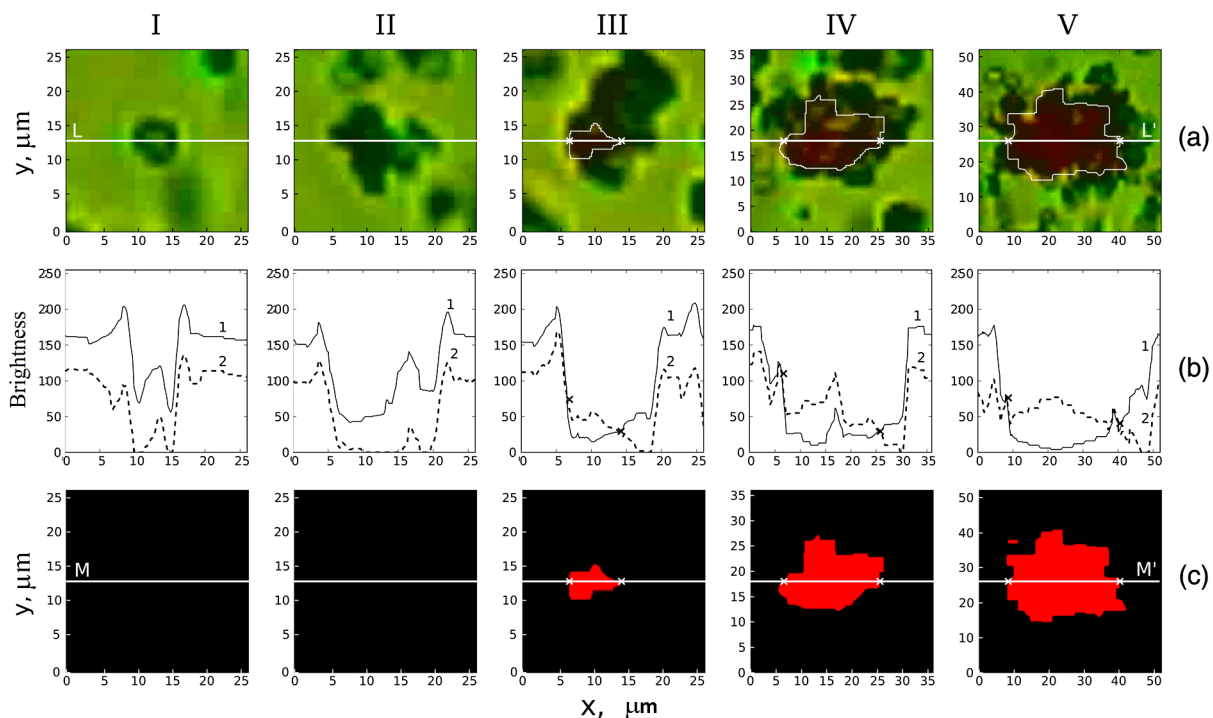


Fig. 4 The set of images and brightness distribution: (a) the raw images of erythrocyte (I) and RBC immune complexes of different sizes (II to V); (b) the distribution of brightness: solid line 1— $B(G)$ as a function of coordinate X ; dash line 2— $B(R)$ as a function of X ; (c) binary images of the raw images (a), the line M-M' corresponds to the line L-L' in raw images (a).

Table 2 The experimental conditions.

Parameters	Variations	Optimum
Ratio blood-serum	—	1:10
Level of the first blood dilution by saline (taking into consideration the volume of serum)	—	1:25
Duration of ultrasonic action upon blood-serum mixture	15 to 120 s	100 s
Duration of a sample incubation after ultrasonic standing wave (USW) action	1 to 4 min	3 to 4 min
Final blood dilution in the testing fluid	1:50 to 1:300	1:150

S_{ai} —the area of i 'th agglutinate, where i is its number (positive reaction of agglutination) and S_{fj} —the area of j 'th RBC-formation, j is its number (negative reaction). The computer program developed allowed us not only to estimate the areas S_{ai} and S_{fj} , but also to calculate the quantity of agglutinates and RBC formations of different sizes. Hence, it was possible to define the distribution of agglutinates and RBC formations in sizes (areas). The same program provided summation of the agglutinate areas $S_a = \sum S_{ai}$ or the areas of RBC formations $S_f = \sum S_{fj}$ for a specified number of snapshots for each sample probe. The comparison of S_a and S_f allows to determine the resolving power of the method (device) from $r = S_a/S_f$.

5 Experimental Results and Discussion

To obtain maximum of resolution r , a series of preliminary experiments were fulfilled with a variation of a number of experimental parameters. The limits of the parameter's variations and some of their optimal magnitudes (when r tends to maximum) are presented in Sec. 2; they were discussed in Ref. 13. On the whole, the limits of the parameters and their optimal values are summarized in Table 2.

The optimal conditions found were used to investigate blood samples of different donors. Every blood sample was analyzed on the basis of four video records for each agglutinating serum (50 image frames in a video). Thus, for each blood sample under analysis, four types of serum, 800 image frames were produced. However, not all of the frames were processed by computer program, but only those in which the same cells and agglutinates

were not repeated (viewed). That is, we have processed only those frames that were separated from each other by such an interval of time during which the erythrocytes and their agglutinates registered in one image frame had enough time to leave the field of view of microscope and not to become fixed in the next frame. The number of chosen image frames was experimentally defined as 144 of the total 800 for each blood sample. Taking into account that each of the frames as a rule had several agglutinates simultaneously, the statistics of sample collection was, thus, quite complete.

The results of measurements for four donor blood samples of different group types are summarized in Table 3. The experimental results presented in each of the cells in Table 3 correspond to the magnitude of the integral agglutinate or RBC-formation area carried out by four video records for each blood-serum pair (combination).

In Table 3, the fundamental impossibility of agglutination for some blood-serum pairs is marked by bold values of the experimental results: a low magnitude of resolution r in nearly all the Table 3 cells ($0 \leq r \leq 5$). At the same time, r is higher enough in the cases when the reaction of agglutination takes place: $r > 100$ and as a rule r close to 1000 and higher. The results presented in Table 3 encourage us to introduce the threshold magnitude of r , which should permit to distinguish positive reaction in respect to the negative one quite accurately.

6 Conclusion

The possibility to introduce a new criterion that may help to differentiate positive reaction of RBC agglutination from negative one was demonstrated theoretically and experimentally. The criterion is based on R and G components comparison of RGB decomposition of optical images of a blood-serum mixture sample by a digital microscopy method. This approach is accompanied by a corresponding computer processing technique and preliminary sampling technique based on ultrasonic standing wave activation of the blood-serum solution.

The proposed method was tested experimentally on the example of monitoring of agglutinates in flows. Encouraging experimental results were obtained in respect to the resolving power of the method. Though the proposed method was realized for dynamic (flow) blood group determination, it may be applied for other diagnostic modalities as well. The approach increases the reliability of RBC agglutinates detection and, hence, blood group typing. The results may be used to develop the apparatus for automated determination of human blood group.

Table 3 The experimental results.

Blood groups studied	Types of agglutinating serum							
	$O_\alpha(I)$ (anti A+B)		$A_\beta(II)$ (anti B)		$B_\alpha(III)$ (anti A)		ABO(IV)	
	S_{a1}	r_1	S_{a2}	r_2	S_{a3}	r_3	S_f	r_4
O(I)	71	2.5	42	1.5	16	0.6	28	1
A(II)	64,213	3380	22	1.1	20,748	1092	19	1
B(III)	9899	146	298,326	4387	341	5.0	68	1
AB(IV)	11,745	734	9459	591	14,233	890	16	1

Acknowledgments

We are thankful to Professor Valery V. Tuchin for reading the manuscript and his valuable advice.

References

1. G. N. Vyas, "Simultaneous human ABO and RH(D) blood typing or antibody screening by flow cytometry," U.S. Patent 5,776,711 (1998).
2. N. Tatsumi, I. Tsuda, and K. Inoue, "Trial ABO and Rh blood typing with an automated blood cell counter," *Clin. Lab Haematol.* **11**(2), 123–130 (1989).
3. J. Murai et al., "Quantitative analysis of Lewis antigens on erythrocytes by flow cytometry," *Clin. Chim. Acta.* **226**(1), 21–28 (1994).
4. Muranyi et al., "Blood typing apparatus," U.S. Patent 4,533,638 (1985).
5. V. A. Doubrovski et al., "Laser space scanning in flow cytometry," *Tsitologiya* **41**(1), 104–108 (1999).
6. V. A. Doubrovski et al., "Laser space scanning for flow particles counters and analyzers," *Instrum. Exp. Techn.* **42**(2), 245–248 (1999).
7. T. J. Mercolino and K. J. Reis, "Simultaneous determination of forward and reverse ABO blood group," U.S. Patent 6,955,889 (2005).
8. D.-S. Kim and T.-H. Kwon, "Microfluidic biochip for blood typing based on agglutination reaction," U.S. Patent 2008/0085551A1 (2008).
9. C. F. Battrell et al., "Microfluidic apparatus and methods for performing blood typing and crossmatching," U.S. Patent 2010/0112723 A1 (2010).
10. D.-S. Kim and T.-H. Kwon, "Microfluidic biochip for blood typing based on agglutination reaction," U.S. Patent 7,718,420 B2 (2010).
11. Y. A. Ganilova, V. A. Doubrovski, and I. V. Zabenkov, "The resolving power of the flowing method to register the process of human erythrocytes agglutination in vitro on the base of correlation analysis of microphotographs," *Proc. SPIE* **7999**, 799903 (2011).
12. V. A. Doubrovski, Y. A. Ganilova, and I. V. Zabenkov, "Application of a spectrally filtered probing light beam and RGB decomposition of microphotographs for flow registration of ultrasonically enhanced agglutination of erythrocytes," *Opt. Spectrosc.* **115**(2), 218–227 (2013).
13. St. R. Anthony, "A simplified visible/near-infrared spectrophotometric approach to blood typing for automated transfusion safety," MS Thesis, North Carolina State University, Raleigh, North Carolina (2005).
14. J. B. Lambert, "A miniaturized device for blood typing using a simplified spectrophotometric approach," MS Thesis, North Carolina State University, Raleigh, North Carolina (2006).
15. S. Narayanan et al., "Ultraviolet and visible light spectrophotometric approach to blood typing: objective analysis by agglutination index," *Transfusion* **39**(10), 1051–1059 (1999).
16. S. Narayanan et al., "UV-visible spectrophotometric approach to blood typing II: phenotyping of subtype A2 and weak D and whole blood analysis," *Transfusion* **42**(5), 619–626 (2002).
17. V. A. Doubrovski and K. N. Dvoretzki, "Detection of ultrasonic agglutination of erythrocytes in vitro by the method of elastic light scattering," *Opt. Spectrosc.* **89**(1), 99–102 (2000).
18. A. A. Dolmashkin and V. A. Doubrovski, "Blood group typing on the basis of digital imaging of sedimentation of erythrocytes and RBC agglutinates," *Biomed. Eng.* **46**(2), 65–70 (2012).
19. V. A. Doubrovski, A. A. Dolmashkin, and I. V. Zabenkov, "Blood grouping based on recording the elastic scattering of laser radiation using the method of digital photography," *Quantum Electron.* **42**(5), 409–416 (2012).
20. K. Nakamura et al., "Agglutination assay method in porous medium layer," U.S. Patent 0,317,126 A1 (2010).
21. T. Takakura and T. Shibuya, "Agglutination image automatic judging method by MT system device program and recording medium," U.S. Patent 2010/0119132 A1 (2010).
22. V. A. Doubrovski and K. N. Dvoretzki, "Ultrasonic wave action upon the red blood cell agglutination in vitro," *Ultrasound Med. Biol.* **26**(4), 655–659 (2000).
23. V. A. Doubrovski, K. N. Dvoretzki, and A. E. Balaev, "Investigation of mechanism of erythrocytes aggregation enhancement by ultrasonic field," *Acoust. Phys.* **50**(2), 146–155 (2004).
24. A. Chung, P. Birch, and K. Ilagan, "A microplate system for ABO and Rh(D) blood grouping," *Transfusion* **33**(5), 384–388 (1994).
25. P. D. Mintz et al., "Application of the inverniss blood grouping system for semiautomated ABO and D testing of patents' samples," *Immunohematology* **10**(2), 60–63 (1994).
26. V. J. Twersky, "Absorption and multiple scattering by biological suspension," *Opt. Soc. Am.* **60**, 1084–1093 (1970).
27. W. B. Gratzler and N. Kollias, "Tabulated molar extinction coefficient for hemoglobin in water," <http://omlc.ogi.edu/spectra/hemoglobin/index.html>.

Valeri A. Doubrovski received his MS in physics from Saratov State University, Russia, in 1965 and his PhD in optics from Saratov State University, Russia, in 1978. He is the head of Biomedical Physics Department of Saratov State Medical University since 1994. His research interests are the development of methods to register spontaneous and induced aggregation of human blood cells *in vitro* and to use it in practice to create medical laboratory apparatus.

Yuliya A. Ganilova received her MS in biophysics from Saratov State University, Russia, in 2000. Since 2005, she is a senior lecturer of Biomedical Physics Department of Saratov State Medical University, Russia. Her research interests are the investigation of blood flow microcirculation in capillaries *in vivo* and the development of flow cytometric method to the problems of blood group typing.

Igor V. Zabenkov received his MS in optics from Saratov State University, Russia, in 2006 and his PhD in optics in 2010. Since 2011, he is a senior lecturer of Biomedical Physics Department of Saratov State Medical University, Russia. His research interests are in optical properties of nanocomposite materials—light scattering and absorption, luminescence; mathematical modeling of light scattering by disperse media; digital photo imaging; and its application to the problems of biomedical investigations and laboratory techniques.